ELSEVIER

Catalysis Today 68 (2001) 173–182

CATALYSIS TODAY

www.elsevier.com/locate/cattod

Synthesis of anatase TiO_2 supported on porous solids by chemical vapor deposition

Zhe Ding [a], Xijun Hu [b,*], Po L. Yue [b], Gao Q. Lu [a], Paul F. Greenfield [a]

[a] *Department of Chemical Engineering, University of Queensland, Brisbane, Qld 4072, Australia*
[b] *Department of Chemical Engineering, Hong Kong University of Science and Technology, Clear Water Bay, Kowloon, Hong Kong*

Abstract

Coating anatase TiO_2 onto three different particle supports, activated carbon (AC), γ-alumina (Al_2O_3) and silica gel (SiO_2), by chemical vapor deposition (CVD) was studied. The effect of the CVD synthesis conditions on the loading rate of anatase TiO_2 was investigated. It was found that introducing water vapor during CVD or adsorbing water before CVD was crucial to obtain anatase TiO_2 on the surface of the particle supports. The evaporation temperature of precursor, deposition temperature in the reactor, flow rate of carrier gas, and the length of coating time were also important parameters to obtain more uniform and repeatable TiO_2 coating. High inflow precursor concentration, high CVD reactor temperature and long coating time tended to cause block problem. Coating TiO_2 onto small particles by CVD involved both chemical vapor deposition and particle deposition. It was believed that the latter was the reason for the block problem. In addition, the mechanism of CVD process in this study included two parts, pyrolysis and hydrolysis, and one of them was dominant in the CVD process under different synthesis route. Among the three types of materials, silica gel, with higher surface hydroxyl groups and macropore surface area, was found to be the most efficient support in terms of both anatase TiO_2 coating and photocatalytic reaction.

Keywords: CVD; Anatase; Particle support; Photocatalysis; TiO_2

1. Introduction

Chemical vapor deposition (CVD) is an old technique with over one century history in the ceramic industry [1]. It becomes popular again because it shows potential application in synthesizing advanced semiconductor materials [2]. TiO_2 is one of the most common semiconductor materials manufactured from CVD process. Due to its high dielectric constant, the TiO_2 thin film obtained by CVD can be applied in solar cells, ferroelectric materials, photoelectrochemical cells, etc. Under most circumstances, the coating was made on flat/cylindrical and smooth surface where dense and uniform coating can be obtained. There are few reports [3,4] using CVD to coat TiO_2 on particle surface, particularly small particles in the range of hundreds of micrometers. It is more difficult to get a good coating on particles because the precursor has to disperse through inter-particle gaps and diffuse into the internal pore structure.

TiO_2 in anatase crystal form is widely accepted as the most active materials in photocatalytic oxidation of organic compounds in water [5–9]. Coating TiO_2 on small particles, therefore, can be used in wastewater treatment and water purification because they can be easily filtered and recovered from the treated water. Furthermore, since they are suspended in the solution, the mass transfer problem is eliminated, leading to

* Corresponding author. Tel.: +852-2358-7134; fax: +852-2358-0054.
E-mail address: kexhu@ust.hk (X. Hu).

0920-5861/01/$ – see front matter
PII: S0920-5861(01)00298-X

higher efficiency than thin TiO_2 film coated on reactor wall or fixed support.

Many precursors can be used in TiO_2 coating by CVD, including organic precursors, such as titanium tetra-isopropoxide (TTIP) [4,10–14] and inorganic precursors, such as titanium tetrachloride [3,15–17], tetranitratotitanium [18]. Mixed precursors can also be used, such as TTIP with titanium tetrachloride [19], and some novel precursors, e.g. TTIP stabilized with a chelating alkoxide [20]. Among various precursors, TTIP and titanium tetrachloride are the most popular ones. In this study, TTIP was chosen as the precursor, because it is less reactive with water than titanium tetrachloride, hence easy to handle. The evaporation temperature is relatively low, and there is no need for oxygen supply in order to produce TiO_2. In addition, there is no contamination from chlorine in the final products, though the role of chlorine in the application is not very clear. The disadvantage of TTIP is the low deposition rate, which can be improved by using vacuum system. In this work, the conditions in the synthesis of anatase TiO_2 supported on particles were experimentally studied. The performance of the developed TiO_2 supported on porous particles as photocatalyst was investigated in the photo-oxidation of phenol.

2. Experimental

2.1. CVD apparatus and procedures

The reactor for CVD synthesis was a quartz tube, which was inserted into a tubular furnace in order to get the desired coating temperature. Since the supports were small particles, there was a porous quartz filter annealed at the end of the tube to prevent blowing out of the particles. TTIP was kept in a different container and heated by water bath to increase the evaporating rate. Nitrogen was bubbled through the container under different flow rates and carried TTIP into the reactor. The whole system was under vacuum. A schematic diagram of the reactor is shown in Fig. 1.

The support materials were activated carbon (Norit Row 0.8 Supra, $\frac{1}{32}$ in. cylindrical extrudate), γ-Al_2O_3 (WHA-217, 50–80 mesh) and silica gel (Aldrich Davisil, 60–100 mesh). Except silica gel used as supplied, the other two supports were washed by deionised water, followed by soaking in 5% HCl solution with constant shaking for 24 h and further washed by deionised water to neutral pH. Three synthesis routes were tried: (I) the supports were degassed at

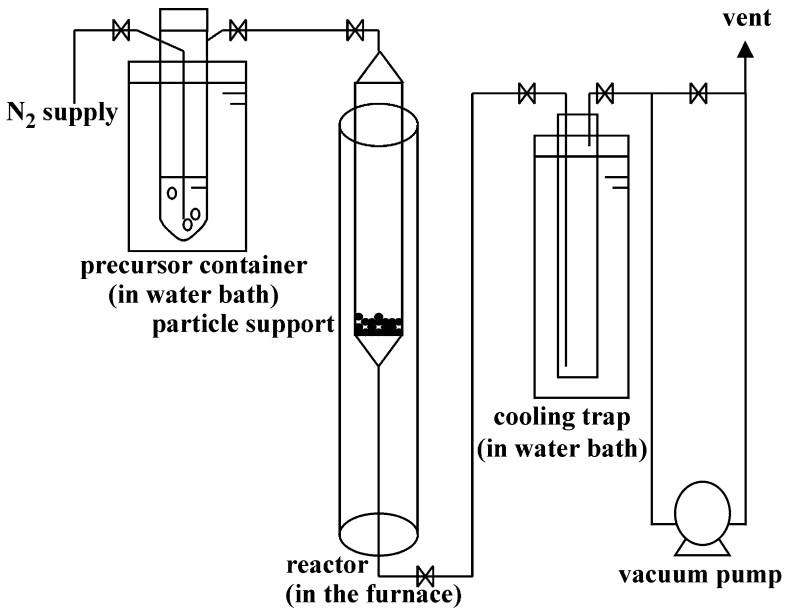

Fig. 1. Schematic diagram of the CVD system.

Table 1
Preparation conditions of anatase TiO_2 coating by CVD

Type of support	Synthesis route	Temperature of precursor (°C)	Flow rate (ml/min)	Temperature of reactor (°C)	Coating time (h)	Anatase peak area by XRD
AC	(I)	100	300	300	8	6222
AC	(I)	40	120	600	24	–
AC	(II)	25	300	200	4	–
AC	(II)	80	120	300	4	–
AC	(III)	100	150	500	10	1764
AC	(III)	80	60	200	10	6914
AC*	(III)	40	60	200	10	3075
Al_2O_3	(I)	25	300	600	60	Block
Al_2O_3	(I)	40	300	600	10	Block
Al_2O_3	(I)	25	60	600	60	6532
Al_2O_3	(I)	40	300	300	10	Block
Al_2O_3	(I)	40	120	300	10	1001
Al_2O_3	(I)	80	120	300	6	–
Al_2O_3	(I)	80	200	300	10	Block
Al_2O_3	(I)	80	90	300	20	Block
Al_2O_3	(II)	25	300	200	4	477
Al_2O_3	(II)	80	120	200	4	1955
Al_2O_3	(III)	40	60	200	9.5	7414
Al_2O_3	(III)	40	60	200	2	954
Al_2O_3*	(III)	40	60	200	4	2575
SiO_2	(I)	80	30	300	3	1144
SiO_2	(I)	80	60	300	3	1931
SiO_2	(III)	80	30	300	3	1069
SiO_2	(III)	80	30	300	5	882
SiO_2	(III)	80	30	300	11	4919
SiO_2	(III)	80	60	300	3	1747
SiO_2*	(III)	80	60	300	4.5	2336
SiO_2	(III)	80	60	300	9.5	4553

* Samples for BET surface area analysis and photocatalytic activity comparison.

300°C for 3 h, then the precursor was introduced into the CVD reactor by carrier gas under vacuum for a given period of time; (II) at the end of the process (I), isolated the precursor, evacuated the reactor for 10 min and then introduced water vapor into the reactor by bubbling nitrogen through a water container without vacuum; (III) the supports (for alumina), after degas, were left in saturated water vapor for half-an-hour, or wet supports (for activated carbon and silica gel) were dried for 20 min at 110°C, then the precursor was introduced under vacuum first at room temperature for 10 min and then increased to the desired temperature. After the CVD process, all the samples using alumina and silica gel as supports were calcined at 500°C for 3 h in air flow, while samples using activated carbon as support were calcined in nitrogen flow. In addition to the different synthesis routes, the temperature of the precursor and the reactor, the flow rate of nitrogen, and the length of the deposition time were also varied. The preparation conditions of different samples are summarized in Table 1.

2.2. Characterization of samples

The presence of TiO_2 in anatase crystal form in different samples was detected by X-ray powder diffractometer (XRD) (Philips PW 1830, Cu Kα radiation). The amount of anatase TiO_2 was represented by the peak area in XRD diagram.

Nitrogen adsorption/desorption of the support materials was performed on ASAP 2000 (Micromeritics). All the samples were degassed at 300°C for 3 h

before the analysis. The surface area and macropore surface area were calculated by BET and *t*-plot method, respectively. The pore size distribution was determined by BJH method.

The element concentration of TiO_2 on the external surface of silica gel sample was measured by X-ray photoelectron spectroscopy (XPS) method (Physical Electronics, PHI 5600). The particle sample was loaded onto the holder without any pretreatment. Fast scan was first made to detect the type of the elements on the surface of the sample. Then slow scan was performed in each element, C (1s), O (1s), Si (2s) and Ti (2p), range.

Morphology of the small TiO_2 particles on the larger support particles was detected by transmission electron microscope (TEM) (JEOL 2010 HREM). Since the particle was too big for the holder, the sample was ground into fine powders first, then dispersed in methanol solution to get better separation.

The photocatalytic activities of different samples were determined through the degradation of phenol in water. The photoreactor was cylindrical with one UV light tube (Philips, 8 W ultra violet fluorescent tube, 356 nm) inserted in the center. Oxygen was bubbled through from the bottom to suspend the catalyst. The total volume of the solution was 150 ml and the input phenol concentration was 20 ppm. After mixing the catalyst with the phenol solution for 1 h, the light was turned on and it was treated as the starting point ($t = 0$) of the reaction and the corresponding phenol concentration was recorded as C_0. The concentration of phenol was measured by the standard 4-aminoantipyrine calorimetric method.

3. Results and discussion

3.1. Effect of preparation conditions on anatase TiO_2 coating

Table 1 presents the preparation conditions of samples with different supports. The changing trend of anatase TiO_2 amount on each type of support material under different conditions is represented by the anatase peak area in XRD diagrams. Four parameters, temperature of the precursor, flow rate of the carrier gas, temperature of the reactor and the coating time were varied in order to determine the optimum conditions for a good TiO_2 coating.

3.1.1. Synthesis route (I)

Synthesis route (I) was first tried in this study. From Table 1, it is clear that for supports of AC and Al_2O_3, this is not an effective method to get an anatase TiO_2 coating. For AC, no anatase phase was detected by XRD analysis. While for Al_2O_3, under most conditions, after CVD reaction, a thin layer of white fine powders was generated on the top of the Al_2O_3 particle layer. The XRD analysis of these powders showed that they were pure TiO_2 in anatase phase. Only two samples have no such block phenomenon. While comparing the synthesis conditions of these two samples with the others (Table 1), it is seen that the first sample was prepared under low precursor temperature and low flow rate. These two parameters determined that there were less TTIP introduced into CVD reactor under the same period of time. Although the coating time was fairly long, 60 h, no block problem was observed. For the second sample, both precursor temperature and flow rate were increased. Since the coating time was shortened, such increase in the TTIP inflow concentration did not lead to block problem. However, further increasing the precursor temperature and flow rate, particularly for flow rate at 300 ml/min, resulted in the production of the TiO_2 thin layer. Under these conditions, TTIP was introduced at high inflow concentration and before they could reach the top of the Al_2O_3 particle layer, part of the TTIP would undergo pyrolysis and transfer into titania fine particles, which were hard to diffuse into the Al_2O_3 particle layer, causing the block problem. Higher reactor temperature also facilitated the pyrolysis of TTIP, thus had more chance to produce titania block layer when the inflow TTIP concentration was high.

For the first TiO_2/AC sample in Table 1, it is seen that the anatase peak area is very high. It should be pointed out that for this sample, both the temperature of the precursor (100°C) and the flow rate of carrier gas (300 ml/min) were very high, while the temperature of the reactor (300°C) was relatively low. Under such condition, the coating was more like a liquid phase coating instead of gas phase coating. If the temperature of the reactor, on the other hand, was also high (500–600°C), TiO_2 fine particles would be formed

quickly and the block phenomenon could happen. In addition, the size of the particle supports was also important for titania coating. For smaller particle size support, TTIP had longer retention time in the CVD reactor, and thus had more chances to produce titania fine particles or react with the support surface. In this study, Al_2O_3 particles were smaller than AC particles, therefore, they were easier to be blocked, while for AC particles, precursor seemed just passing by rather than adsorbed on the surface of the AC particles and the final product had little or no anatase TiO_2 coated.

Compared with AC and Al_2O_3, the anatase TiO_2 coating on SiO_2 was better. The particle size of SiO_2 was similar to Al_2O_3. However, there was no block problem for SiO_2 supports. The main reason was because the inflow TTIP concentration was lower and coating time was much shorter. Anatase TiO_2 coating could be obtained after 3 h for SiO_2, while for Al_2O_3 under similar conditions, there was no detectable anatase TiO_2 even after a coating time of 6 h. This difference was believed to come from the difference of the surface hydroxyl groups between the two support materials. The surface of SiO_2 had more chemisorbed hydroxyl groups, which were active sites for the TTIP hydrolysis reaction. Therefore, compared with Al_2O_3, TTIP was more efficiently adsorbed and reacted on the SiO_2 surface. In addition, higher surface area of SiO_2 was also beneficial for the coating process. The nitrogen adsorption/desorption isotherms and pore size distributions for the two supports are shown in Figs. 2 and 3, respectively.

The surface area of SiO_2 (294 m^2/g) was larger than that of Al_2O_3 (179 m^2/g). More importantly, for both materials, the surface area was mainly macropore surface area. This was an advantage when compared with AC material, which had the highest surface area (1011 m^2/g) but mainly in micropore range (4.8–19 Å). The average pore size in SiO_2 (150 Å) was bigger than that in Al_2O_3 (100 Å), which made the TTIP molecule easier to transfer onto the macropore surface of SiO_2 support. For both SiO_2 and Al_2O_3 samples, the surface area slightly dropped after CVD reaction, which became 259 m^2/g for TiO_2/SiO_2 and 153 m^2/g for TiO_2/Al_2O_3. In addition, there was little change in the pore size distribution. This implies that the porous structure of the support was well preserved after CVD reaction and most of the TiO_2 was coated onto the external or macropore surface of the supports.

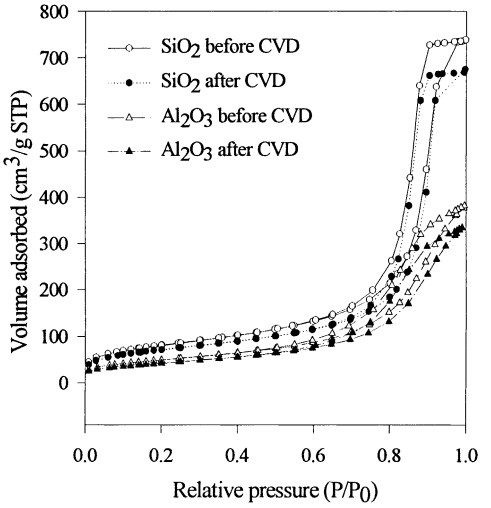

Fig. 2. Nitrogen adsorption/desorption isotherm of SiO_2 and Al_2O_3 supports before and after CVD treatment.

3.1.2. Synthesis route (II)

Introducing water vapor into the CVD reactor after the precursor had contacted the support for long enough time, was also tried for AC and Al_2O_3 supports. This would be helpful if there was any TTIP adsorbed on the support but had not been decomposed. TTIP would be hydrolyzed by the water vapor and TiO_2 was formed. From Table 1, it can be seen that there is still no anatase TiO_2 on AC supports. This implies that AC had little adsorption capacity

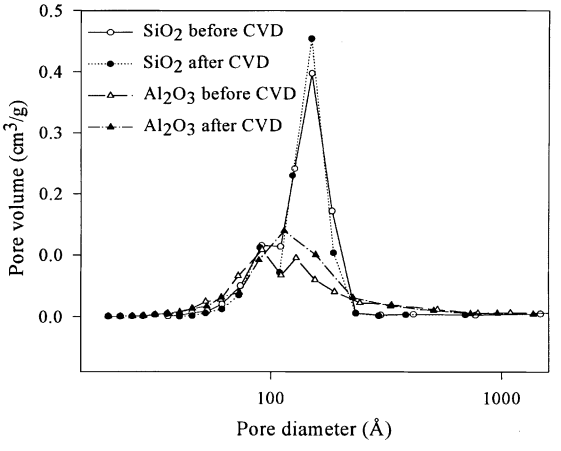

Fig. 3. Pore size distribution of SiO_2 and Al_2O_3 supports before and after CVD treatment.

for TTIP. However, for Al_2O_3 supports, anatase TiO_2 coating was obtained at a much shorter coating time. Thereafter, the block problem was solved. Comparing the two TiO_2/Al_2O_3 samples, it can be seen that increasing the temperature of the precursor significantly increased the amount of coated anatase TiO_2. The second synthesis route was superior over the first one, since it reduced the consumption of precursor and the coating time, and increased the amount of anatase TiO_2 coated onto the support. However, the reaction had one more step, and before introducing water vapor, the system should be blown with N_2 thoroughly in order to remove any precursor residue inside the reactor. A similar but simpler synthesis route, therefore, was developed.

3.1.3. Synthesis route (III)

The success of introducing water vapor after precursor deposition on Al_2O_3 support confirms that the presence of water or hydroxyl groups is important for the generation of anatase TiO_2 coating. Therefore, adsorption of water onto the surface of the supports before introducing precursor was tried. All three types of supports were left in saturated water vapor. It was found that less water adsorbed on SiO_2 than Al_2O_3 and nearly no water was adsorbed on AC. Hence, for AC and SiO_2, water was first added to the supports, then the supports were put into the oven and dried partially.

The coating results were quite promising. For all three types of supports, anatase TiO_2 coating was successfully obtained and the block problem was eliminated. The XRD results for all three supports were shown in Fig. 4. The four groups of numbers associated with the XRD curves refer to the evaporation temperature (°C), flow rate of carrier gas (ml/min), deposition temperature (°C) and coating time (h), respectively. The peak at 25.28° refers to anatase TiO_2 and there is no rutile TiO_2 detected, which has a peak at 27.45°. The calculated anatase peak area for each sample is listed in Table 1.

From Table 1, it is seen that increasing the coating time was beneficial in increasing the amount of anatase TiO_2 coated and the flow rate had similar but much less effect on anatase TiO_2 coating. However, it is also observed that for AC sample, increasing the temperature of the reactor had an adverse effect on the amount of the anatase TiO_2 coated. As discussed before, higher reactor temperature had more chance to form a TiO_2 block layer. Under high temperature, the trend for the pyrolysis of the precursor was stronger, leading to the generation of fine TiO_2 powders. Considering the big AC particle size, part of these TiO_2 powders might go through the inter-particle space of the AC supports instead of depositing onto the support surface, resulting in less amount of anatase TiO_2 coated.

3.2. Mechanisms of TiO_2 coating by CVD in three synthesis routes

Generally, TiO_2 coating by CVD process can be expressed by the following equations [21]:

$$\mathrm{TTIP\,(g)} + \mathrm{M\,(g)} \rightarrow \mathrm{I\,(g)} \quad (1)$$

$$\mathrm{I\,(g)} + \mathrm{S^*} \rightarrow \mathrm{I\,(a)} \quad (2)$$

$$\mathrm{I\,(a)} \rightarrow \cdots \rightarrow \mathrm{P\,(g)} + \mathrm{TiO_2\,(s)} \quad (3)$$

where M represents a collision partner, I the intermediate species, S^* the vacant surface site on the support and P the gas phase product. The reaction starts by the collision of two gas phase molecules, e.g. TTIP with another TTIP or N_2, and generating a more active intermediate species I (g). They will in turn react with the surface active site and undergo pyrolysis to produce deposited TiO_2 and the gas phase by-product, P (g), which will leave the surface.

In this study, the TiO_2 block phenomenon indicates that TTIP can not only follow the above mechanism and deposit TiO_2 onto the surface of the support, but also undergo pyrolysis and generate TiO_2 powder before it reaches the surface of the support. The gas phase particle nucleation was also observed on flat surface [22]. However, in most cases, it happened under atmospheric pressure [2]. By introducing vacuum, or for low-pressure CVD, it is believed that Eqs. (1)–(3) are the dominant reactions. Furthermore, it is difficult to observe this phenomena when using a flat surface as the support. Since after these fine TiO_2 powders are generated, they will settle down on the surface and it is hard to distinguish them from those powders coming from Eq. (3). On the other hand, while using small particles as the support, diffusion problem is more serious than flat supports. It is more difficult for those fine TiO_2 powders to be transferred

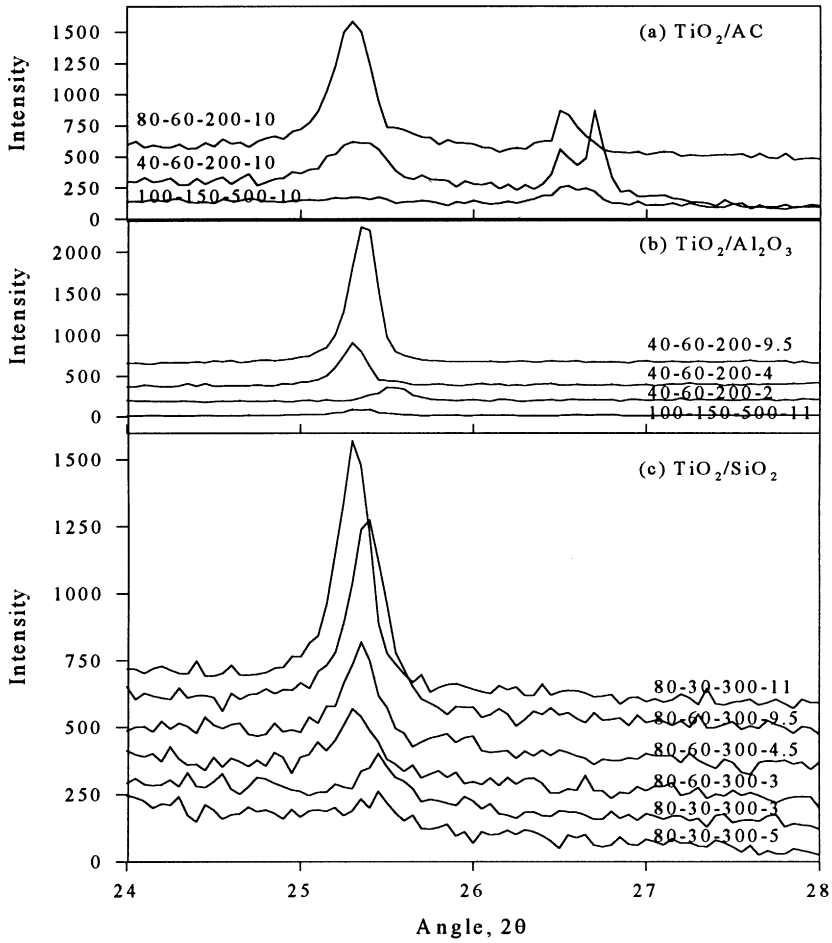

Fig. 4. XRD diagram of TiO_2 coated on three supports synthesized from route (III) (samples are represented by the value of the synthesis parameters as: precursor temperature–flow rate–reactor temperature–coating time): (a) TiO_2/AC, (b) TiO_2/Al_2O_3 and (c) TiO_2/SiO_2.

to the surface of the particles, particularly to the bottom part of the particle support layer, and most of them will stay on the top of the layer, leading to the block problem. Therefore, the TiO_2 coating on small particles by CVD is a process with combination of TTIP vapor deposition, Eqs. (1)–(3) and TiO_2 powder deposition:

$$\mathrm{TTIP\,(g)} \rightarrow \cdots \rightarrow \mathrm{TiO_2\,(s)} + \mathrm{C_3H_6\,(g)} + \mathrm{H_2O\,(g)} \quad (4)$$

Eqs. (1)–(4) represent the simple mechanism for the synthesis route (I). The water produced in the gas phase will hydrolyze TTIP and cause more TTIP to be transferred to TiO_2 before it contacts the support. It can well explain why the block problem happened often for Al_2O_3 supports. Long coating time coupled with high inflow TTIP concentration provided a good condition for the pyrolysis of TTIP in the main flow, leading to the TiO_2 block on the top of the particle support layer.

As for synthesis route (II), adding water vapor after TTIP, the reaction, Eqs. (1)–(4), for synthesis route (I) is still applied. In addition to the pyrolysis of TTIP to produce TiO_2, TTIP adsorbed on the surface can also undergo hydrolysis:

$$S/TTIP\,(a) + H_2O \rightarrow \cdots \rightarrow S/TiO_2\,(s) + C_3H_7OH \quad (5)$$

or

$$S\text{–}O\text{–}Ti(OC_3H_7)_3 + H_2O \rightarrow \cdots \rightarrow S\text{–}OH + TiO_2\,(s) + C_3H_7OH \quad (6)$$

It can be seen that in synthesis route (II), it is easier to produce TiO_2. The time for the reaction is shorter and the reaction condition is milder than synthesis route (I). However, it has one prerequisite, which the precursor needs to be able to be adsorbed or chemically bonded on the surface of the support before introducing water vapor. Therefore, if synthesis route (I) cannot work for one kind of support, it is very much possible that synthesis route (II) cannot work, either. In this study, AC is an example.

For synthesis route (III), similar to synthesis route (II), the reaction mechanism also contains two parts, hydrolysis and pyrolysis. It is believed that hydrolysis plays a dominant role in the generation of TiO_2 coating. In this case, water is introduced first and the surface of the support is hydrolyzed before the precursor is blown through. Therefore, the hydrolysis part should be revised as

$$2S + 2H_2O \rightarrow S\text{–}OH\cdots H + S/H_2O\,(a) \quad (7)$$

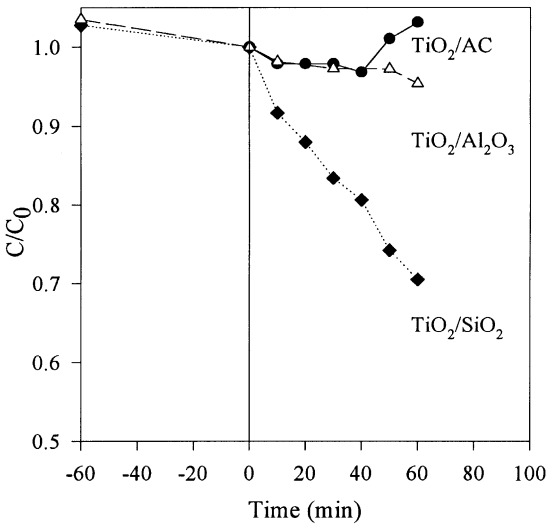

Fig. 5. Comparison of photocatalytic activities in the photooxidation of phenol among three samples (negative value in time axis represents the mixing period before turning on the UV lights).

$$S\text{–}OH\cdots H + S/H_2O\,(a) + TTIP \rightarrow \cdots \rightarrow S/TiO_2\,(s) + C_3H_7OH \quad (8)$$

Compared with synthesis route (II), there is less limitation on the characteristics of the support and anatase TiO_2 can be coated successfully on all three types of materials.

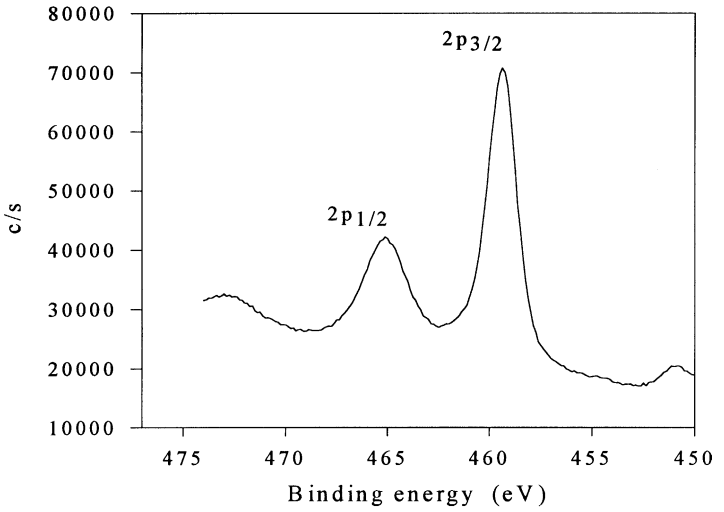

Fig. 6. XPS Ti(2p) of TiO_2/SiO_2 sample.

3.3. Photocatalytic activity of catalysts in the degradation of phenol aqueous solution

The photocatalytic activities of anatase TiO_2 coated samples were tested using phenol as the model organic compound. The results of three samples (with $*$ symbols in Table 1) are shown in Fig. 5.

It can be seen that samples with Al_2O_3 and AC as support materials have little or no activity in the degradation of phenol. AC is a strong adsorbent for phenol. In this study, the input phenol concentration for TiO_2/AC was 400 ppm instead of 20 ppm. After mixing for 18 h, most of the phenol was adsorbed on the catalyst, the phenol concentration in the solution was reduced to 18 ppm and there was no further degradation after turning on the lamp. It should be noted that because of the strong adsorption of phenol on AC supports, it was difficult to determine the exact amount of phenol being photocatalytically degraded. The reason why the phenol concentration was not changing, or even increasing, might be that AC acted as a supplier for phenol. The pre-adsorbed phenol might be released into the solution continuously to offset the phenol oxidized. For TiO_2/Al_2O_3 and TiO_2/SiO_2, very little phenol (<3%) was adsorbed before the photocatalytic reaction and TiO_2/SiO_2 showed higher activity than TiO_2/Al_2O_3. Because TiO_2/SiO_2 had a higher surface area, the anatase TiO_2 was better dispersed on SiO_2 support. For the photocatalytic reaction, surface area of the photocatalyst is critical to obtain a high activity, which explains why TiO_2/SiO_2 is more efficient than TiO_2/Al_2O_3. Another reason is the difference in the primary anatase TiO_2 crystallite size, which can be calculated from XRD curves. The anatase TiO_2 sizes were 50 nm for TiO_2/Al_2O_3 and 13 nm for TiO_2/SiO_2, respectively. Smaller crystal size means better distribution of anatase TiO_2 on the supports, thereafter, has more active sites for the photocatalytic reaction.

The XPS and TEM analysis results of TiO_2/SiO_2 sample are shown in Figs. 6 and 7, respectively. In Fig. 6, the two peaks, Ti($2p_{3/2}$) and Ti($2p_{1/2}$), at 459 and 465 eV indicate that the titanium cation is in Ti^{4+} covalent state. Therefore, in TiO_2/SiO_2 sample, most titanium existed as TiO_2. Furthermore, the amount of TiO_2 on the external surface of the particle sample can also be obtained through XPS curves, which was 21.6 wt.%, much higher than the bulk anatase TiO_2 concentration in the sample. Therefore, one can

(a)

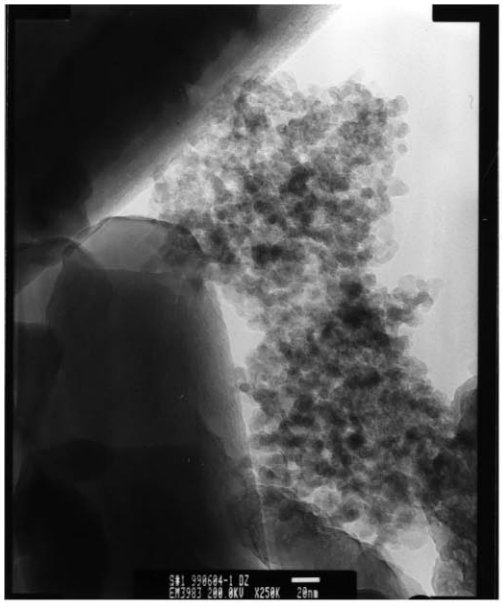

(b)

Fig. 7. TEM micrograph of TiO_2/SiO_2 sample: (a) particle; (b) TiO_2 layer.

conclude that for TiO_2/SiO_2 sample, most anatase crystals distributed on the external surface, which supports the surface area analysis results. In addition, the TEM image shows that the anatase TiO_2 primary particle size is quite uniform and around 10 nm, which agrees well with XRD results.

4. Conclusions

Anatase TiO_2 supported on three different porous particle supports, AC, Al_2O_3 and SiO_2 have been synthesized by CVD method. A high inflow precursor concentration and low CVD reactor temperature led to the liquid phase coating, while a high inflow precursor concentration and high CVD reactor temperature might cause a block problem. In the coating process of anatase TiO_2 onto porous particles by CVD, both TTIP vapor deposition and TiO_2 particle deposition existed. When the condition was beneficial for TiO_2 particle deposition, long coating time would result in block problem. Introducing water vapor onto the support before CVD shortened the deposition time and enhanced the TiO_2 loading rate. Synthesis route (III) was superior over the other two routes and was workable for all three types of materials. The porous structure of the materials was maintained after CVD and anatase TiO_2 particles dispersed mainly on the external or macropore surface of the supports. Among three types of materials, SiO_2 was the best support for coating anatase TiO_2 by CVD and TiO_2/SiO_2 showed the highest activity in the photocatalytic degradation of phenol in water.

Acknowledgements

The authors are grateful for the assistance provided by Ms. P.Y. Cheung in XRD measurements. Financial support from the Research Grants Council of Hong Kong (Project No. HKUST6035/98P), and Australian Research Council is also gratefully acknowledged.

References

[1] H.O. Pierson, Handbook of Chemical Vapor Deposition (CVD): Principles, Technology and Applications, Noyes Publications, Park Ridge, NJ, 1992.
[2] A. Sherman, Chemical Vapor Deposition for Microelectronics: Principles, Technology and Applications, Noyes Publications, Park Ridge, NJ, 1987.
[3] K. Schrijnemakers, N.R.E.N. Impens, E.F. Vansant, Langmuir 15 (1999) 5807.
[4] L. Lei, H.P. Chu, X. Hu, P.L. Yue, Ind. Eng. Chem. Res. 38 (1999) 3381.
[5] R.L. Pozzo, M.A. Baltanas, A.E. Cassano, Catal. Today 39 (1997) 219.
[6] O. Legrini, E. Oliveros, A.M. Braun, Chem. Rev. 93 (1993) 671.
[7] D.F. Ollis, H. Al-Ekabi (Eds.), Photocatalytic Purification and Treatment of Water and Air, Elsevier, Lausanne, 1993.
[8] D.Y. Goswami, J. Solar Energy Eng. 119 (1997) 101.
[9] A.L. Linsebigler, G. Lu, J.T. Yates Jr., Chem. Rev. 95 (1995) 735.
[10] P. Babelon, A.S. Dequiedt, H. Mostefa-Sba, S. Bourgeois, P. Sibillot, M. Sacilotti, Thin Solid Films 322 (1998) 63.
[11] Y.K. Han, T.G. Lee, S.S. Yom, M.H. Son, E.K. Kim, S.K. Min, J.Y. Lee, J. Korean Phys. Soc. 32 (1998) s1538.
[12] Y.K. Han, T.G. Lee, S.S. Yom, M.H. Son, E.K. Kim, S.K. Min, J.Y. Lee, J. Korean Phys. Soc. 32 (1998) s1697.
[13] K.L. Siefering, G.L. Griffin, J. Electrochem. Soc. 137 (1990) 814.
[14] K.L. Siefering, G.L. Griffin, J. Electrochem. Soc. 137 (1990) 1206.
[15] A.Y. Stakheev, C.W. Lee, P.J. Chong, Bull. Korean Chem. Soc. 19 (1998) 530.
[16] C. Pophal, F. Kameda, K. Hoshino, S. Yoshinaka, K. Segawa, Catal. Today 39 (1997) 21.
[17] A. Stabel, A. Caballero, J.P. Espinos, F. Yubero, A. Justo, A.R. Gonzalez-Elipe, Surf. Coat. Technol. 100–101 (1998) 142.
[18] D.C. Gilmer, D.G. Colombo, C.J. Taylor, J. Roberts, G. Haugstad, S.A. Campbell, H.S. Kim, G.D. Wilk, M.A. Gribelyuk, W.L. Gladfelter, Chem. Vap. Deposition 4 (1998) 9.
[19] A. Goosens, E.L. Maloney, J. Schoonman, Chem. Vap. Deposition 4 (1998) 109.
[20] A.C. Jones, T.J. Leedham, P.J. Wright, M.J. Crosbie, K.A. Fleeting, D.J. Otway, P. O'Brien, M.E. Pemble, J. Mater. Chem. 8 (1998) 1773.
[21] Q. Zhang, G.L. Griffin, Thin Solid Films 263 (1995) 65.
[22] P. Tandon, D.E. Rosner, AIChE 42 (1996) 1673.